Comparison of Hypercapnia-Based Calibration Techniques for Measurement of Cerebral Oxygen Metabolism With MRI

Daniel P. Bulte,[1*] Knut Drescher,[1,2] and Peter Jezzard[1]

MRI may be used to measure fractional changes in cerebral oxygen metabolism via a metabolic model. One step commonly used in this measurement is calibration with image data acquired during hypercapnia, which is a state of increased CO_2 content of the blood. In this study some commonly used hypercapnia-inducing stimuli were compared to assess their suitability for the calibration step. The following stimuli were investigated: (a) inspiration of a mixture of 4% CO_2, 21% O_2 and balance N_2; (b) 30-s breath holding; and (c) inspiration of a mixture of 4% CO_2 and 96% O_2 (i.e., carbogen). Measurements of BOLD and cerebral blood flow made on nine subjects during the different hypercapnia-inducing stimuli showed that each stimulus leads to a different calibration of the model. We argue that of the aforementioned stimuli, inspiration of 4% CO_2, 21% O_2 and balance N_2 should be preferred for the calibration as the other stimuli produce responses that violate assumptions of the metabolic model. Magn Reson Med 61:391–398, 2009. © 2009 Wiley-Liss, Inc.

Key words: FMRI; BOLD; arterial spin labeling; ASL; hypercapnia; breath holding; $CMRO_2$

Obtaining structural images of the brain with MRI is a well-established clinical tool. Functional MRI (fMRI) methods are mostly used to localize neuronal activity, by computing how well the measured signal fits to a predicted response (1). Such approaches show "activation" images based on the statistical significance of the fit, thresholded at an arbitrarily level. This localization of neuronal activity is not directly related to the magnitude of the response (2,3). In addition, the signals that are used in fMRI are only indirectly related to the underlying neuronal activation. In clinical applications, however, it is of great interest to have quantitative information about parameters that are directly related to neuronal activation or its associated metabolic demand (4).

A mathematical model that uses MRI data to calculate fractional changes in the cerebral metabolic rate of oxygen consumption ($CMRO_2$) has been proposed (5,6). The $CMRO_2$ response is closely related to neuronal activation because the increased energy demand of the activated neurons is met by an increase in the metabolic rate of O_2 consumption (2). The MRI $CMRO_2$ model requires a calibration step that effectively estimates the maximum possible BOLD fMRI signal change. Typically this is achieved by imaging during a hypercapnia challenge in which the CO_2 content of the blood in increased, although recently an alternative method based on hyperoxia has been suggested and shown to give a higher signal to noise ratio (7).

Hypercapnia is chosen because it is assumed that it increases the cerebral blood flow (CBF) without changing the metabolism (i.e., the $CMRO_2$), thereby providing ideal conditions for the calibration, as outlined below. Several different techniques for inducing hypercapnia have been used in the literature, including (a) breathing CO_2-enriched air (with 21% O_2) (5,8–10); (b) various breath holding tasks (11,12); and (c) breathing a CO_2/O_2 mixture without nitrogen (13,14). However, these techniques may not be equally suitable for calibration of the $CMRO_2$ model. A study that directly compared methods (a) and (b) found that both methods are equally suitable for the calibration of the $CMRO_2$ model (15), yet that study drew this conclusion from CBF measurements that are not in agreement with those reported in references (5,8–10). We, therefore, studied each of these hypercapnia challenges in detail to determine their suitability as a calibration step for $CMRO_2$ measurements with MRI. In particular, we made simultaneous measurements of BOLD and CBF responses during each stimulus, as well as measurements of the end-tidal CO_2 and O_2 levels to determine whether the stimuli induced markedly different states and calibrations in the subjects. The different stimuli were also compared theoretically by considering the physiological implications of each stimulus in relation to the MRI $CMRO_2$ model.

BACKGROUND THEORY

Model for Estimating Cerebral Oxygen Metabolism using MRI

A model that allows a calculation of the $CMRO_2$ from BOLD and cerebral blood flow (CBF) image data was proposed in references (5,6). Briefly, Fick's principle states that:

$$CMRO_2 = CBF \times 4[Hb^{tot}](Y_{art} - Y_{ven}), \qquad [1]$$

where $[Hb^{tot}]$ is the total concentration of hemoglobin in the blood, and Y_{art} and Y_{ven} are the O_2 saturation fractions of arterial and venous blood, respectively (2). Because $Y_{art} \cong 1$, the concentration of deoxyhemoglobin (deoxyHb) in the venous blood, can be interpreted as being $[Hb^{tot}]\ (1 - Y_{ven})$, which is proportional to $CMRO_2$/CBF. If it is assumed that the magnetic susceptibility difference between

[1]FMRIB Centre, Department of Clinical Neurology, University of Oxford, United Kingdom.

[2]Department of Physics, University of Oxford, United Kingdom.

Grant sponsor: Medical Research Council (UK); Grant sponsor: The Wingate Foundation.

*Correspondence to: Daniel P. Bulte, FMRIB Centre, John Radcliffe Hospital, Headington, Oxford OX3 9HN United Kingdom. E-mail: bulte@fmrib.ox.ac.uk

Received 31 October 2007; revised 19 September 2008; accepted 22 September 2008.

DOI 10.1002/mrm.21862
Published online in Wiley InterScience (www.interscience.wiley.com).

blood and tissue ($\Delta\chi$) is proportional to [deoxyHb] (5), then:

$$\Delta\chi \propto CMRO_2/CBF. \quad [2]$$

Previous studies (5,16) have shown that it is possible to empirically relate the change in effective transverse relaxation rate during neuronal activation, $\Delta R_2^* = \Delta(1/T_2^*)$, to the cerebral fractional blood volume (CBV) and $\Delta\chi$ as:

$$\Delta R_2^* \propto CBV\Delta\chi^{\beta} - CBV_0\Delta\chi_0^{\beta}, \quad [3]$$

where the "0" subscripts indicate baseline values and the exponent parameter β has been reported as 1.5 at 1.5 Tesla (T), but is estimated to be 1.3 when scaled for its field dependence at 3T (17–19) for this study. By then expressing the BOLD signal equation as a Taylor expansion it is possible to combine the above equations to give (5):

$$1 - \frac{BOLD}{BOLD_0} \propto \left[\frac{CBV}{CBV_0}\left(\frac{CBF}{CBF_0}\right)^{-\beta}\left(\frac{CMRO_2}{CMRO_{2|0}}\right)^{\beta} - 1 \right]. \quad [4]$$

Grubb's formula, given by $CBV/CBV_0 = (CBF/CBF_0)^{\alpha}$ (and for which previous studies have found $\alpha = 0.38$) (20–22) may then be used to eliminate CBV/CBV_0 from Equation [4]. Defining the fractional change in BOLD signal with respect to baseline as $\Delta BOLD/BOLD_0 \equiv BOLD/BOLD_0 - 1$, and similarly $\Delta CBF/CBF_0 \equiv CBF/CBF_0 - 1$, gives:

$$\frac{\Delta BOLD}{BOLD_0} = M\left[1 - \left(\frac{\Delta CBF}{CBF_0} + 1\right)^{\alpha-\beta}\left(\frac{CMRO_2}{CMRO_{2|0}}\right) \right]^{\beta}. \quad [5]$$

In this equation, M is the maximum theoretical BOLD signal change. By inspection it may be seen that once M is determined, it is possible to evaluate changes in $CMRO_2$ from measurements of CBF and BOLD signal changes. To determine this calibration constant, M, $\Delta CBF/CBF_0$, and $\Delta BOLD/BOLD_0$ must be recorded during some stimulus that does not lead to a change in neuronal activation (so that $\Delta CMRO_2/CMRO_{20} \equiv CMRO_2/CMRO_{20} - 1 = 0$), but does lead to changes in the CBF and BOLD signal. Such iso-metabolic changes may be caused by hypercapnia. During hypercapnia the BOLD signal increases due to the CBF increases, which dilute the concentration of paramagnetic deoxyHb in the venous blood, thus providing the necessary calibration data.

MATERIALS AND METHODS

A total of 13 nonsmoking healthy volunteers were recruited to the study. Of these individuals, only nine (all male, aged 26 ± 6) have been included in the study. For the other four subjects a variety of problems were encountered that related to the demanding stimulus protocol: two subjects experienced claustrophobia in the MRI scanner; a third subject continuously hyperventilated such that the level of CO_2 in his blood did not increase during the stimuli; and the fourth subject was eliminated due to head movement that correlated with the stimulus protocol. Each subject gave informed consent and the protocol was approved by the appropriate research ethics committee.

Stimulus Protocol

Details of the stimulus protocol are illustrated in Figure 1. The three CO_2 stimuli were (a) breathing of a mixture of 4% CO_2, 21% O_2 and balance N_2 ("4% CO_2 in air") for 3 min, (b) repeated periods of breath holding/normal breathing for 30 s/30 s, and (c) breathing of 96% O_2 and 4% CO_2 ("carbogen") for 3 min. Longer breath holds would have been desirable because they would have allowed more arterial spin labeling (ASL) images to be acquired during the stimulus (only one ASL pair is acquired every 9 s). However, some subjects already had difficulties when practicing their 30-s breath holds. To enable an estimation of end-tidal expired O_2 and CO_{2o} at the end of the breath hold, subjects were instructed to hold their breath after an inspiration. Each stimulus was executed twice during the 42 min 9 s of data recording for each subject. This yielded additional signal-to-noise and ensured that any drifts in the apparatus would be detected. The gas stimuli were chosen to have a duration of 3 min to be comparable to previous studies (9). The order of stimulus presentation was pseudo-randomized across the group so that each subject received each stimulus during both the first and second half of the scan time, but in different orders across the group, for example, abccab, cbaacb, etc.

Breath hold instructions were given by means of a visual cue (Presentation, Neurobehavioral Systems Inc., Albany, CA) with well-controlled timing (correct to 1 ms), which was projected onto a screen at the end of the MRI scanner. A 30-s count down was given for the first breath hold in a series of six breath holds, and a 5-s warning for the subsequent breath holds. The details of the gas delivery system are illustrated in Figure 2. Subjects wore a mask that covered their nose and mouth (8920 Series, Hans Rudolph Inc., Kansas City, MO), connected to a filter (A). A small tube (B) delivered samples of the expired and inspired gases to CO_2 and O_2 analyzers (not shown; Models CD-3A and S-3A, AEI Technologies, Pittsburgh, PA). The respiratory data were recorded at intervals of 0.05 s, and showed that there was no measurable re-breathing. Tubes C, D, E,

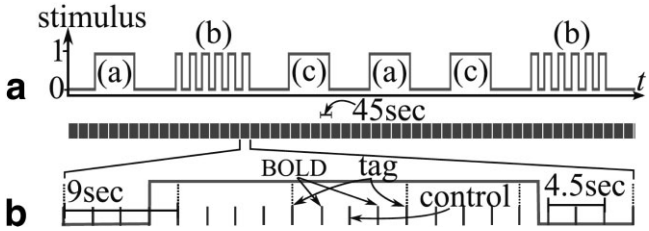

FIG. 1. **A:** An example time course of the stimuli, which are (a) 4% CO_2, 21% O_2 and balance N_2 for 3 min ("4% CO_2 in air"), followed by 3 min of normal air, (b) six periods of 30-s breath holds each followed by a 30-s normal breathing (giving a total breath hold time of 3 min), (c) 4% CO_2 and 96% O_2 ("carbogen") for 3 min, followed by 3 min of normal air. **B:** The interleaved BOLD-CBF pulse sequence during one breath hold: Every 9 s, two BOLD images are acquired (separated by 4.5 s) as well as one CBF-"tag" and one CBF-"control" image.

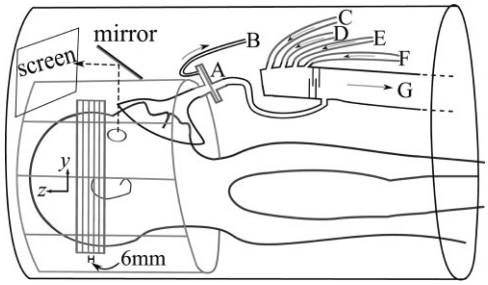

FIG. 2. Respiratory monitoring and gas delivery system in relation to the scanner hardware and stimulus presentation. See text for a full description.

and F delivered the following gases: $CO_2/O_2/N_2$ at 5%/21%/74%, CO_2/O_2 at 5%/95%, pure O_2, and normal air with negligible CO_2 content. Tubes were flooded with gases before each scan. The relative rate at which each of these gases was delivered determined the overall gas mixture that the subject breathed. The mixture of gases was administered at a total rate of 30 L/min (more than twice the rate of normal inhalation of air), so that excess gases built up in the exhaust path G and no re-breathing occurred. The five slices that were imaged are also indicated in the figure.

Details of Pulse Sequence

Images were acquired on a 3T MRI scanner (TIM Trio, Siemens Medical Solutions, Erlangen, Germany), using a 12-channel head radiofrequency receive coil. An interlaced BOLD/pulsed ASL sequence was used to collect T_2*-weighted conventional EPI images and macrovascular-crushed Q2TIPS (23,24) cerebral perfusion images in the following scheme: [ASL tag image/BOLD image/ASL control image/BOLD image]$_n$. 281 repetitions of this cycle (562 total BOLD and 281 ASL difference images) were acquired per run. BOLD measurements had TR/TE = 4.5 s/32 ms, and ASL experiments had TR/TE/TI = 4.5 s/23 ms/1.4 s. In both BOLD and ASL, 5 slices were acquired per TR, with $4 \times 4 \times 6$ mm^3 voxel dimensions and a 64×64 imaging matrix. MP-RAGE T_1-weighted images were acquired for registration of the EPI information to anatomical data, with $1 \times 1 \times 1$ mm^3 voxel dimensions and a 192×256 imaging matrix.

Data Analysis

The data were analyzed with tools from the FMRIB Software Library (FSL). This software (i) aligned the images and corrected for head motion (25); (ii) extracted those voxels that correspond to brain matter from images that also contain the skull and skin (26); (iii) filtered the time course signal such that only frequencies with a period shorter than 6 min were retained to reduce scanner and subject-specific drift; and (iv) fitted an expected BOLD response curve to the BOLD data for every voxel using a General Linear Model (27,28). The regions of interest (ROIs) were defined as all activated voxels with $Z>3$ for the BOLD data, and $Z>1$ for the ASL data during the 4% CO_2 in air stimulus, and these 2 ROIs were then applied to the other 2 stimuli (BOLD ROI to BOLD data, ASL ROI to ASL data) so that the number of voxels for each dataset was constant. Activated voxels for each image set were selected rather than the union or intersection so as not to bias the results by including spurious data or omitting significant voxels. The thresholds were selected to create ROIs of as similar size as possible for each sequence taking into account the difference in SNR. The activations are limited primarily to grey matter regions, and due to the low SNR of the ASL data it would not be practical to further reduce the ROIs to specific brain regions as then the total number of voxels would be too small for an analysis such as this. The median percentage signal change in the ROIs was then found for each stimulus. Using the median rather than the mean gives a lower weighting to artifactual outlier activations.

The predicted responses were calculated by convolution of a top-hat function of unit height (nonzero only during the stimulus, as in Fig. 1A) with a gamma-variate hemodynamic response function, as described in reference (29). The parameters that were used for the gamma-variate hemodynamic response function were as follows: mean lag of 60 s and a SD of 60 s for gas stimuli, and a mean lag of 30 s and a SD of 10 s for the breath holds. Respiratory tasks, and breath holding in particular, are known to have stimulus correlated motion as a potential confound, thus during the motion correction phase of the analysis, any subject who exhibited any stimulus-correlated-motion event of greater than 0.5 mm in the *x*- or *y*-directions or greater than 1.0 mm in the *z*-direction was excluded from the study. One volunteer exhibited head motion that correlated significantly with the breath hold paradigm, and their data were, therefore, excluded from further analysis. None of the other subjects exhibited significant head motion that correlated with breath holding, although the majority of subjects exhibited some small motions with some of the breath holding events. Bite bars could potentially be used to reduce the possibility of these motions acting as a confound.

Analysis of the ASL data was split into two separate steps. First, the region of interest was defined as all activated voxels, which were identified in a similar manner to that described above for the BOLD data, except that the regressors were modified by including an additional term that alternated between ±1 to account for the tag/control nature of the ASL data, and the statistical threshold for activation was lowered to $Z = 1.0$. This lowering accounted for the lower signal-to-noise ratio of the ASL data compared with the BOLD data, and enabled a comparable number of activated voxels to be produced.

Second, the ASL images were loaded into Matlab after steps (i) and (ii) had been performed and after the ASL difference data had been calculated. In Matlab, the median signal change from baseline of the activated voxels was then found by (a) computing the median signal of all activated voxels at every time point, (b) computing the mean of the median signal during stimulus periods and (c) comparing this mean signal to the baseline signal to give *dS*, the percent change in raw ASL difference-signal. For the CO_2 in air and breath hold epochs $\Delta dS/dS$ is equivalent to the $\Delta CBF/CBF_0$ (30).

Table 1
End Tidal Values for Oxygen and Carbon Dioxide for Each Subject During Normal Breathing and Each Gas Stimulus*

Subject	Air		4% CO2 in air		Breath hold		Carbogen	
	ET CO2	ET O2	ET CO2	ET O2	ET CO2	ET O2	ET CO2	ET O2
1	5.15 ± 0.10	15.03 ± 0.45	5.98 ± 0.08	15.42 ± 0.33	6.22 ± 0.20	12.18 ± 0.88	5.60 ± 0.06	78.65 ± 1.42
2	5.85 ± 0.18	14.35 ± 0.46	6.53 ± 0.05	15.10 ± 0.46	6.73 ± 0.24	12.37 ± 0.79	5.95 ± 0.05	78.23 ± 3.11
3	5.40 ± 0.19	15.40 ± 0.45	6.45 ± 0.10	15.27 ± 0.36	6.63 ± 0.08	12.57 ± 0.79	6.03 ± 0.08	79.38 ± 3.79
4	5.10 ± 0.17	15.63 ± 0.34	6.28 ± 0.15	15.38 ± 0.31	6.27 ± 0.20	13.03 ± 0.28	5.78 ± 0.10	83.63 ± 0.55
5	5.63 ± 0.23	14.80 ± 0.91	6.68 ± 0.21	15.43 ± 0.51	6.60 ± 0.19	13.22 ± 0.53	5.98 ± 0.08	90.82 ± 0.53
6	5.27 ± 0.37	16.10 ± 0.65	6.15 ± 0.26	15.83 ± 0.36	6.22 ± 0.19	13.82 ± 0.62	5.52 ± 0.26	74.93 ± 1.15
7	5.30 ± 0.01	16.17 ± 0.15	5.70 ± 0.06	16.67 ± 0.15	6.13 ± 0.06	13.77 ± 1.67	5.83 ± 0.26	57.00 ± 0.57
8	5.75 ± 0.19	14.83 ± 0.43	6.40 ± 0.32	15.57 ± 0.69	6.38 ± 0.08	13.48 ± 0.81	6.37 ± 0.16	70.48 ± 1.10
9	5.38 ± 0.05	16.03 ± 0.06	6.35 ± 0.24	16.80 ± 0.55	6.23 ± 0.16	14.08 ± 1.31	6.65 ± 0.23	94.08 ± 0.81
mean	5.43	15.37	6.28	15.72	6.37	13.17	5.97	78.58

*Values are means for the two blocks of stimulus per subject ± SD. The bottom row is the mean of the tabulated mean values across all subjects above.

The conversion from changes in ASL signal to changes in CBF is further complicated for the data collected during carbogen, because this stimulus changes the level of O_2 in the blood, leading to changes in the relaxation times of the net magnetization in blood (31). Because the ASL signal equation is sensitive to blood relaxation times (32) the $\Delta CBF/CBF_0$ calculated in steps (i–iii) for carbogen was, therefore, corrected as described in Bulte et al. (33).

RESULTS

The mean end tidal values for oxygen and carbon dioxide are presented in Table 1. All three stimuli led to hypercapnia, indicated by a statistically significant increase ($P < 0.05$) in the percentage of end-tidal expired CO_2 (which is an indicator of the level of CO_2 dissolved in the blood (34)). The breath holds and 4% CO_2 in air result in similar end tidal CO_2 levels, as designed, however, the same fraction of inspired CO_2 ($FiCO_2$) in balance oxygen results in a lower end tidal CO_2 value. This is likely due to the tendency toward hyperventilation induced by hyperoxia which would blow off more CO_2. The different effects of each stimulus on the end tidal oxygen levels display the significant differences between the techniques, most notably that breath holding induces a significant decrease in comparison to normal air and 4% CO_2 in air, whereas carbogen induces a substantial increase.

The resulting changes in the CBF and BOLD signal with respect to baseline are listed in Table 2 and plotted in Figure 3. Activation in response to the different stimuli occurred predominantly in grey matter for BOLD and CBF images, as reported previously for gas stimuli and hypercapnia (11,29,33). Example activation maps for a single slice from a single representative subject are shown in Figure 4. From this it can been seen that the number of activated voxels is of a similar order across the three conditions and between the two imaging techniques, the trends discussed in the following paragraph can also be discerned.

The data from the individual subjects, as well as the intersubject mean values, showed that each hypercapnic state had a distinctive signature: The BOLD signal change was largest during inspiration of carbogen and smallest during breath holding. The observed differences in ASL signal change between the different states of hypercapnia are less distinct than the BOLD values as a result of the low signal-to-noise ratio in the CBF images (and the resulting need to lower the *Z*-score threshold for activation as described in the data analysis section), yielding large SDs in the calculated ΔCBF and *dS* values. Nevertheless, a trend

Table 2
Fractional Changes in BOLD Signal, ASL Signal (for Carbogen Only), and CBF With Respect to Baseline in Percent for Each Stimulus*

Subject	Carbogen			4% CO_2 in air		Breath hold (BH)	
	BOLD	ΔASL	ΔCBF	BOLD	ΔCBF	BOLD	ΔCBF
1	3.70	7.70	19	2.60	46.00	1.00	19.90
2	4.41	7.70	19	1.86	21.10	−0.81	8.70
3	2.89	16.30	28	2.54	33.20	1.45	22.30
4	4.00	16.30	28	2.52	33.50	1.23	21.70
5	4.71	14.00	27	2.89	33.30	1.41	23.40
6	2.76	13.60	26	2.25	26.20	1.38	15.50
7	3.58	4.40	15	2.11	31.34	1.70	11.90
8	4.00	9.88	20	2.38	21.28	1.45	1.09
9	4.11	11.12	23	2.74	27.90	1.57	12.94
Mean	3.8 ± 0.65	11.22 ± 4.15	22.78 ± 4.74	2.43 ± 0.32	30.42 ± 7.61	1.15 ± 0.76	15.27 ± 7.41

*In this study "carbogen" is the gas mixture of 96% O_2 and 4% CO_2, and "4% CO_2 in air" is the gas mixture of 4% CO_2, 21% O_2, and balance N_2. Value and error are intersubject mean ±1 SD of the intersubject variation.

in the ΔCBF and *dS* of the individual subjects is present: the ΔCBF was smallest during breath holding and largest during inspiration of 4% CO_2 in air. In Figure 3, the line with $\Delta CMRO_2/CMRO_{20} = 0$ has been drawn (in grey). The *M* value (defined in Eq. [5]) used for this plot was calculated from the intersubject mean of the 4% CO_2 in air stimulus.

DISCUSSION

The results in Figure 3 obtained at 3T can be compared with other hypercapnia studies at other field strengths such as those presented in Figure 5, all of which were performed at 1.5T. These cannot be displayed on the same set of axes as the BOLD responses (ΔR_2*) are not directly comparable at different field strengths, however, the positions of each data point relative to the zero metabolic change contour can be determined. The isometabolic contour for zero change in metabolism in Figure 5 was calculated using the values for 5% $FiCO_2$ by Kastrup et al. (15). The results of studies by Kim et al. (10), Davis et al. (5), and Stefanovic et al. (8), although spanning a range of $FiCO_2$ values, are all very close to the calculated $\Delta CMRO_2/CMRO_{20} = 0\%$ contour, as would be expected for isometabolic stimuli. Significantly, the data from Kastrup et al. (15) suggest that breath holding (data point marked with a ○) and inspired 5% CO_2 in air (•) have the same effect on ΔR_2* and CBF within experimental error.

In the present study, there is a clear distinction between the BOLD and CBF responses to the three different hypercapnia stimuli. To interpret exactly what the cause of these differences is, it is essential to consider the physiological effects of each, as well as the different effects that each will have on magnetization relaxation. Figure 6 shows the mean end tidal measurements averaged across the 9 subjects and the error bars show 1 SD (these results are also given in tabular form in Table 1). As can be seen in this figure, all three stimuli cause an increase in the end tidal partial pressure of carbon dioxide (PCO_2) to very similar degrees, all within experimental error, as the experiment was designed to achieve. The significant difference between the stimuli is only apparent upon inspection of the end tidal oxygen levels shown in the lower panel of Figure 6. Here we can observe that although the 4% CO_2 in air causes only minimal change in the partial pressure of oxygen (PO_2), both breath holding and carbogen (off the scale in Fig. 6) significantly alter the measured PO_2.

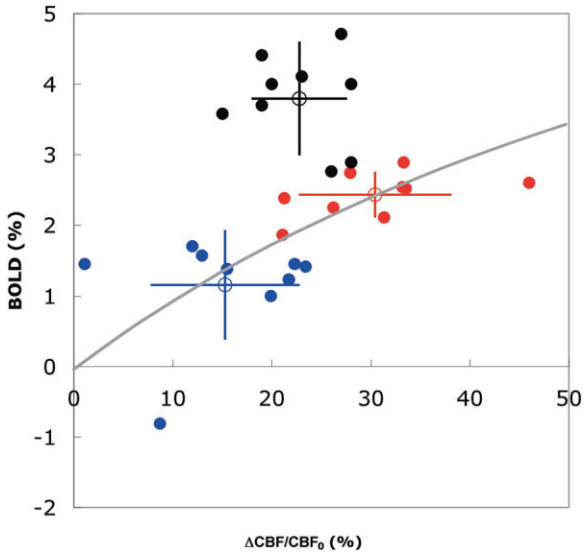

FIG. 3. Individual subject data from Table 2 is shown. Error bars correspond to ±1 SD; black, red, and blue markers correspond to measurements during inspiration of carbogen, 4% CO_2 in air, and breath holding, respectively. The nine different markers represent the nine different subjects. Large circles indicate the intersubject mean of each stimulus. The gray line is a plot of Equation [5] at zero change in $CMRO_2$. The calibration constant *M* was calculated from the intersubject mean of the 4% CO_2 in air.

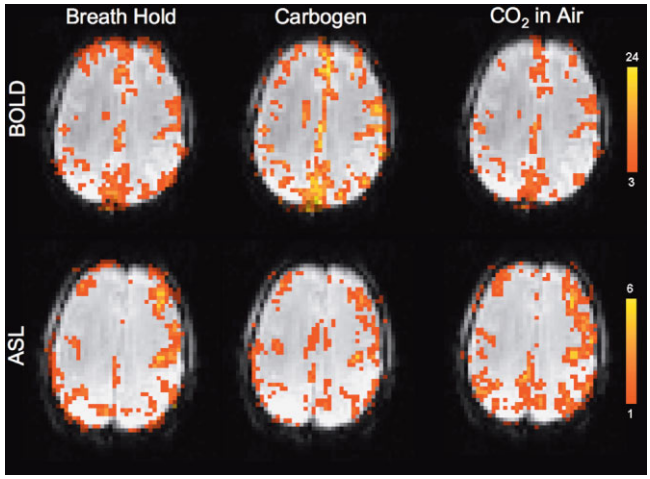

FIG. 4. BOLD and ASL activation maps in a single slice for a single representative subject. The top row are the BOLD activation maps for the three stimuli, and the bottom row are the ASL activation maps. The scales on the right show the color range of the *Z*-scores for each sequence's results.

The mean result across all subjects from the 4% CO_2 in air stimulus was used to calculate the isometabolic curve in Figure 3. For this stimulus, the results for all subjects lie close to the isometabolic curve, which may be representative of the differences between subjects individual physiologies and breathing patterns. This supports the link between isometabolic changes in CBF and their effect on the BOLD signal. As the end tidal oxygen levels for this stimulus were essentially unchanged from normal air, there should be minimal effect on relaxation times, the BOLD signal, or independent effects of the oxygen on flow or metabolism.

Conversely, when considering the carbogen results it is easy to see that the large increase in PO_2, causes a substantial increase in the venous saturation, resulting in a substantial additional increase in the BOLD signal. Likewise the similar CO_2 levels cause a similar increase in CBF to the 4% CO_2 in air stimulus, however, the vasoconstrictive effect of the excess oxygen causes this response to be slightly muted in comparison (33). The CBF changes calculated for the carbogen stimulus have taken the changes in relaxation times due to the dissolved oxygen into account. The BOLD signal measured when using carbogen as a stimulus thus violates the assumption that the signal

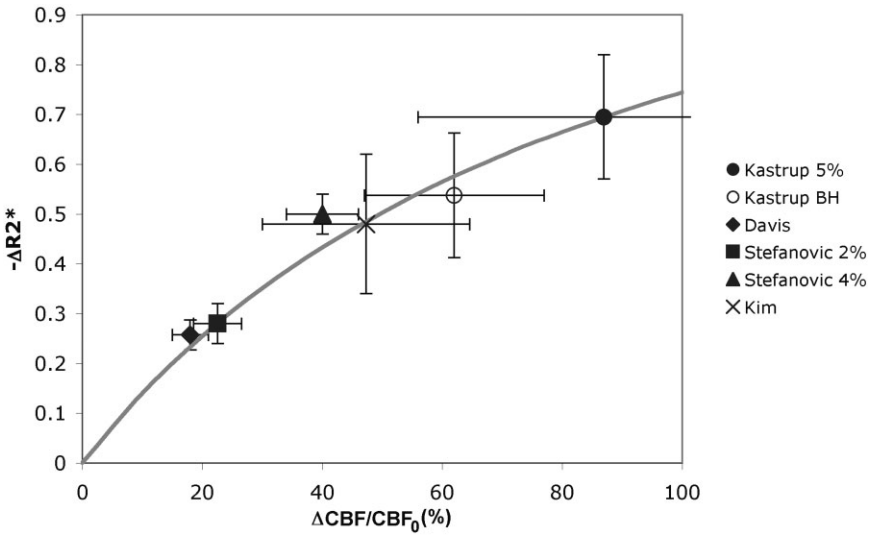

FIG. 5. ΔR_2^* versus $\Delta CBF/CBF_0$ data from studies at 1.5T from Stefanovic et al. (8) who used 2% and 4% CO_2 in air, Kim et al. (10) who used 5% CO_2 in air, Davis et al. (5) who used 5% CO_2 in air, and Kastrup et al. (15) for which breath holds are marked with ○, 5% CO_2 in air with •. The gray line illustrates the iso-metabolic contour for $\Delta CMRO_2/CMRO_{20} = 0\%$ as in Figure 3, calculated from the 5% CO_2 data by Kastrup et al. Error bars are ±1 SD of the intersubject variation.

changes are purely a result of an isometabolic change in CBF, and so carbogen is not suitable as a calibration agent.

The most interesting result presented here is the data from the breath hold stimulus. Our result shows the mean breath hold response lying directly on the zero metabolism change curve calculated using the data from the 4% CO_2 in air stimulus. Upon comparison with results from other studies (Fig. 5), it can be seen that breath hold data by Kastrup et al. lies similarly close to the isometabolic line, however, the error bars show it to be statistically indistinguishable from their result for 5% CO_2 in air, suggesting that breath holding is an equivalent challenge for calibration purposes. In contrast, our results show breath holding to be statistically different to the 4% CO_2 in air stimulus. Most importantly though, the end tidal measurements show that the levels of PCO_2 achieved during the breath hold were equivalent to the 4% CO_2 in air stimulus, which would suggest that the BOLD and CBF responses should have been the same. The difference between the two challenges may be revealed in the end tidal oxygen measurements which show the that breath hold challenge results in a significant reduction in PO_2. Figure 7 shows the measured respiratory gases from a single subject during one 30-s inspiration breath hold. The increase in CO_2 is apparent, however, so is the associated decrease in O_2. Just as the difference in the oxygen levels in the blood dominate the location of the carbogen data on the BOLD-CBF plane, so the location for the breath hold must be likewise affected. If this is the case then the decreased oxygen could be artifactually decreasing the measured BOLD response, which would otherwise be equivalent to the 4% CO_2 stimulus. However, one would expect that a decrease in arterial PO_2 (PaO_2) would induce a further increase in CBF in response, rather than a lower CBF increase.

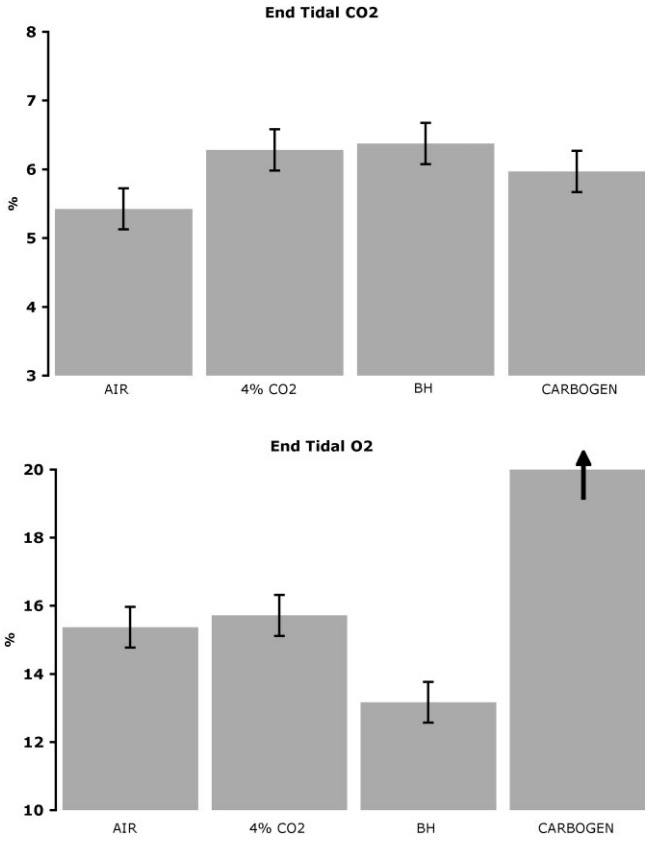

FIG. 6. Mean end tidal measurements of carbon dioxide (top) and oxygen (bottom), expressed as percentages of atmospheric pressure averaged across all 9 subjects, error bars represent ±1 SD for the group. The oxygen result for carbogen is off the scale as shown by the arrow, the exact vales for these are shown in Table 1.

The reason for this discrepancy is most likely the physical differences between a 3-min inspiration gas stimulus and a series of six 30-s breath holds. The temporal response of the respiratory and vascular systems is quite slow, it can take up to 2 min for changes in end tidal oxygen and carbon dioxide to plateau even at mild levels of change, and the greater the degree of change, the longer it takes to stabilize. Also the change in partial pressures during a breath hold are constantly changing as more CO_2 is being produced and more oxygen extracted throughout the breath hold, whereas the $FiCO_2$ and FiO_2 are constant during a gas challenge. As a result, although the analysis of

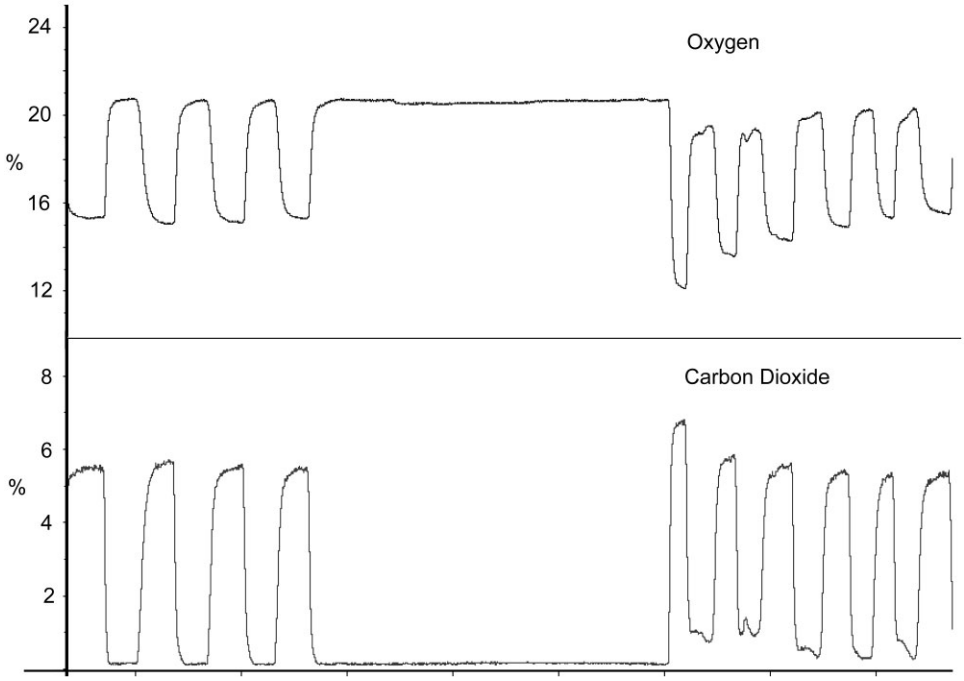

FIG. 7. Measured respiratory gas traces for a single subject during a single 30-s inspiration breath hold, showing the measured changes in oxygen (top) and carbon dioxide (bottom) expressed as percentages of atmospheric pressure, and the significant changes in the gases in the first exhalation after the breath hold.

the expired gases after a breath hold showed a similar CO_2 level to the 4% gas challenge, the dynamics of both the PCO_2 and the vascular changes in response to this may have been very different, and after only 30 s the response is possibly never given a chance to reach the same level as it would over 3 contiguous minutes. There is also the possibility that the reduction in oxygen is causing a change in metabolism, and this change is being masked from the BOLD signal due to the signal change being caused by changes in venous oxygen saturation.

To properly investigate the differences between short and long duration respiratory challenges it would be necessary to use a technique called end-tidal forcing (35), possibly combined with controlled or forced breathing, which would drive the partial pressures to a plateau as quickly as possible so that changes over shorter periods could be compared fairly. Further problems of using breath hold data for calibration of the $CMRO_2$ model are an increased sensitivity to head motion, and discrepancies between whether subjects hold their breath after expiration or inspiration, where the former group will already have a higher level of CO_2 in the blood at the beginning of the breath hold (36). It is also important to recognize the differences between different duration breath holds. Not only will shorter breath holds be easier to tolerate, they will also be less susceptible to correlated head motion. When not using a sequence like the interleaved BOLD/ASL one used here, sufficient data points may be obtained within a shorter period (37,38); however, the degree of change in the partial pressures of oxygen and carbon dioxide will also be reduced. As a result breath holds of different durations cannot be directly compared.

There is also a general concern when using hypercapnia as a calibration agent as recent work has indicated that hypercapnia is not an isometabolic stimulus at all (39). An alternate option is to not use hypercapnia as a calibration step, but to use hyperoxia instead. This is a technique introduced by Chiarelli et al. (7) which involves the inspiration of increased fractions of oxygen to alter the venous oxygen saturation levels. The benefits of this technique, beyond the improved tolerability in comparison to hypercapnia, include the removal of the dependence on the relatively low SNR CBF measurements, and the possibility of using nasal cannula to deliver the oxygen. Cannulae are more comfortable than face masks and allow for the use of bite bars to further reduce the possibility of motion artifacts.

CONCLUSIONS

The most commonly used stimuli for inducing hypercapnia were compared to determine their suitability for calibration of the $CMRO_2$ model. The comparison was based on simultaneous acquisition of BOLD and ASL data during the different stimuli. It was found that if a CO_2-based calibration method is used, the $CMRO_2$ model should be calibrated with measurements of BOLD signal and CBF changes during the inspiration of CO_2-enriched air. On theoretical grounds, neither breath holding nor inspiration of a CO_2/O_2 mixture without nitrogen should be used, as both stimuli can potentially lead to BOLD signal changes that cannot be accounted for within the $CMRO_2$ model.

ACKNOWLEDGMENTS

We thank D. Gallichan (FMRIB, Oxford) and J. Kuijer (VUMC, Amsterdam) for provision of the pulse sequence.

REFERENCES

1. Smith SM, Jenkinson M, Woolrich MW, Beckmann CF, Behrens TEJ, Johansen-Berg H, Bannister PR, De Luca M, Drobnjak I, Flitney DE,

Niazy RK, Saunders J, Vickers J, Zhang Y, De Stefano N, Brady JM, Matthews PM. Advances in functional and structural MR image analysis and implementation as FSL. Neuroimage 2004;23(Suppl 1):S208–S219.
2. Jezzard P, Matthews PM, Smith SM. Functional MRI: an introduction to methods. Oxford: Oxford University Press; 2003.
3. Tofts P. Quantitative MRI of the brain: measuring changes caused by disease. London: John Wiley and Sons Ltd; 2004.
4. An H, Chen Y, Chang L, Lin W. Temporal and spatial evolution of MR derived cerebral metabolic rate of oxygen utilization index in acute middle cerebral artery occlusion stroke rats. In: Proceeding of the 14th Annual Meeting of ISMRM, Seattle, Washington, USA, 2006. (abstract 1471).
5. Davis TL, Kwong KK, Weisskoff RM, Rosen BR. Calibrated functional MRI: mapping the dynamics of oxidative metabolism. Proc Natl Acad Sci U S A 1998;95:1834–1839.
6. Hoge RD, Atkinson J, Gill B, Crelier GR, Marrett S, Pike GB. Investigation of BOLD signal dependence on cerebral blood flow and oxygen consumption: the deoxyhemoglobin dilution model. Magn Reson Med 1999;42:849–863.
7. Chiarelli PA, Bulte DP, Wise R, Gallichan D, Jezzard P. A calibration method for quantitative BOLD fMRI based on hyperoxia. Neuroimage 2007;37:808–820.
8. Stefanovic B, Warnking JM, Pike GB. Hemodynamic and metabolic responses to neuronal inhibition. Neuroimage 2004;22:771–778.
9. Chiarelli PA, Bulte DP, Piechnik S, Jezzard P. Sources of systematic bias in hypercapnia-calibrated functional MRI estimation of oxygen metabolism. Neuroimage 2007;34:35–43.
10. Kim SG, Rostrup E, Larsson HBW, Ogawa S, Paulson OB. Determination of relative CMRO2 from CBF and BOLD changes: significant increase of oxygen consumption rate during visual stimulation. Magn Reson Med 1999;41:1152–1161.
11. Kastrup A, Krüger G, Glover GH, Moseley ME. Assessment of cerebral oxidative metabolism with breath holding and fMRI. Magn Reson Med 1999;42:608–611.
12. Thomason ME, Foland LC, Glover GH. Calibration of BOLD fMRI using breath holding reduces group variance during a cognitive task. Hum Brain Mapp 2007;28:59–68.
13. Vesely A, Sasano H, Volgyesi G, Somogyi R, Tesler J, Fedorko L, Grynspan J, Crawley A, Fisher JA, Mikulis DJ. MRI mapping of cerebrovascular reactivity using square wave changes in end-tidal PCO2. Magn Reson Med 2001;45:1011–1012.
14. Macey PM, Alger JR, Kumar R, Macey KE, Woo MA, Harper RM. Global BOLD MRI changes to ventilatory challenges in congenital central hypoventilation syndrome. Respir Physiol Neurobiol 2003;139(1):41–50.
15. Kastrup A, Krüger G, Neumann-Haefelin T, Moseley ME. Assessment of cerebrovascular reactivity with functional magnetic resonance imaging: comparison of CO2 and breath holding. Magn Reson Imaging 2001;19:13–20.
16. Ogawa S, Lee TM, Barrere B. The sensitivity of magnetic resonance image signals of a rat brain to changes in the cerebral venous blood oxygenation. Magn Reson Med 1993;29:205–210.
17. Edelman RR, Hesselink J, Zlatkin M, Crues J. Clinical magnetic resonance imaging. Philadelphia: Elsevier; 2005.
18. Uludag K, Dubowitz DJ, Yoder EJ, Restom K, Liu TT, Buxton RB. Coupling of cerebral blood flow and oxygen consumption during physiological activation and deactivation measured with fMRI. Neuroimage 2004;23:148–155.
19. Buxton RB. Introduction to functional magnetic resonance imaging. Cambridge: Cambridge University Press; 2002.
20. Grubb RL Jr, Raichle ME, Eichling JO, Ter Pogossian MM. The effects of changes in PaCO2 on cerebral blood volume, blood flow, and vascular mean transit time. Stroke 1974;5:630–639.
21. Rostrup E, Knudsen GM, Law I, Holm S, Larsson HBW, Paulson OB. The relationship between cerebral blood flow and volume in humans. Neuroimage 2005;24:1–11.
22. Mandeville JB, Marota JJA, Kosofsky BE, Keltner JR, Weissleder R, Rosen BR, Weisskoff RM. Dynamic functional imaging of relative cerebral blood volume during rat forepaw stimulation. Magn Reson Med 1998;39:615–624.
23. Luh WM, Wong EC, Bandettini PA, Hyde JS. QUIPSS II with thin-slice TI1 periodic saturation: a method for improving accuracy of quantitative perfusion imaging using pulsed arterial spin labeling. Magn Reson Med 1999;41:1246–1254.
24. Wong EC, Buxton RB, Frank LR. Quantitative imaging of perfusion using a single subtraction (QUIPSS and QUIPSS II). Magn Reson Med 1998;39:702–708.
25. Jenkinson M, Bannister P, Brady M, Smith S. Improved optimization for the robust and accurate linear registration and motion correction of brain images. Neuroimage 2002;17:825–841.
26. Smith SM. Fast robust automated brain extraction. Hum Brain Mapp 2002;17:143–155.
27. Woolrich MW, Ripley BD, Brady M, Smith SM. Temporal autocorrelation in univariate linear modeling of FMRI data. Neuroimage 2001;14:1370–1386.
28. Worsley KJ, Evans AC, Marrett S, Neelin P. A three-dimensional statistical analysis for CBF activation studies in human brain. J Cereb Blood Flow Metab 1992;12:900–918.
29. Rostrup E, Law I, Blinkenberg M, Larsson HBW, Born AP, Holm S, Paulson OB. Regional differences in the CBF and BOLD responses to hypercapnia: a combined PET and fMRI study. Neuroimage 2000;11:87–97.
30. Detre JA, Alsop DC. Perfusion fMRI with arterial spin labeling (ASL). In: Moonen CTW, Bandettini PA, editors. Functional MRI. Heidelberg: Springer-Verlag; 1999. p 47–62.
31. Kennan RP, Scanley BE, Gore JC. Physiologic basis for BOLD MR signal changes due to hypoxia/hyperoxia: separation of blood volume and magnetic susceptibility effects. Magn Reson Med 1997;37:953–956.
32. Buxton RB, Frank LR, Wong EC, Siewert B, Warach S, Edelman RR. A general kinetic model for quantitative perfusion imaging with arterial spin labeling. Magn Reson Med 1998;40:383–396.
33. Bulte DP, Chiarelli PA, Wise RG, Jezzard P. Cerebral perfusion response to hyperoxia. J Cereb Blood Flow Metab 2007;27:69–75.
34. Klinke R, Pape H-C, Silbernagl S. Lehrbuch der Physiologie. Stuttgart: Thieme; 2006.
35. Wise RG, Pattinson KTS, Bulte DP, Chiarelli PA, Mayhew SD, Balanos GM, O'Connor DF, Pragnell TR, Robbins PA, Tracey I, Jezzard P. Dynamic forcing of end-tidal carbon dioxide and oxygen applied to functional magnetic resonance imaging. J Cereb Blood Flow Metab 2007;27:1521–1532.
36. Plathow C, Ley S, Zaporozhan J, Schoebinger M, Gruenig E, Puderbach M, Eichinger M, Meinzer HP, Zuna I, Kauczor HU. Assessment of reproducibility and stability of different breath-hold maneuvres by dynamic MRI: comparison between healthy adults and patients with pulmonary hypertension. Eur Radiol 2006;16:173–179.
37. Handwerker DA, Gazzaley A, Inglis BA, D'Esposito M. Reducing vascular variability of fMRI data across aging populations using a breath-holding task. Hum Brain Mapp 2007;28:846–859.
38. Thomason ME, Burrows BE, Gabrieli JDE, Glover GH. Breath holding reveals differences in fMRI BOLD signal in children and adults. Neuroimage 2005;25:824–837.
39. Zappe AC, Uludag K, Oeltermann A, Ugurbil K, Logothetis NK. The influence of moderate hypercapnia on neural activity in the anesthetized nonhuman primate. Cereb Cortex 2008 [Epub ahead of print].